15th IFK
Proc. of the 15th International Fluid Power Conference <Symposium/Conference>
<DOI>

Power optimization strategy design for electric wheel loader work function with variable speed and pump displacement control

Jiaming Wu[1], Yihan Qiao[1], Feng Wang[1*], Bing Xu[1]

[1] *State Key Laboratory of Fluid Power Components and Mechatronic Systems in the School of Mechanical Engineering, Zhejiang University, Hangzhou, Zhejiang, 310027, China*

[*] *Corresponding author. E-mail address: dieter@zju.edu.cn*

Abstract.

Powertrain electrification is key to decarbonizing mobile machinery like wheel loaders. However, their work functions still rely on centralized valve control, causing significant energy losses. Electro-hydrostatic actuators (EHA) offer a decentralized, efficient alternative but often use fixed-displacement pumps, leading to poor efficiency under high-torque, low-speed conditions. Existing cooperative speed and displacement control are rule-based and neglect system dynamics, limiting optimal effect. This paper proposes a power optimization strategy for electric wheel loader work function with variable speed and pump displacement cooperative control. Offline dynamic programming (DP) first determines globally optimal operating points under typical conditions. Then a real-time optimization strategy is proposed based on the optimal results from DP algorithm. Results show the proposed system achieves a 9.12% reduction in energy consumption compared with the EHA system under the familiar cycle (9.76% for DP system). Under another unfamiliar cycle, the proposed system still has a 4.9% energy consumption reduction, demonstrating its energy-saving potential across various operating conditions.

Keywords. Electro-hydraulic actuator, variable speed and pump displacement control, dynamic programming, distributed hydraulic system, mobile machine.

1. INTRODUCTION

Powertrain electrification has emerged as a pivotal technological pathway for reducing carbon emissions in mobile machinery and represents a major focus of current research [1]. Among various types of electric mobile equipment, wheel loaders have achieved the highest market penetration [2]. Conventional electric wheel loaders typically utilize two electric motors—one for wheel drive and another for the working functions, and the latter consumes a substantial portion of the total battery energy. Although these systems employ high-efficiency electric motors, the working functions often continue to rely on centralized

hydraulic valve control systems [3]. This results in significant throttling losses, reduced overall system efficiency, and limited operational duration per charge [4].

Decentralized hydraulic systems have gained increasing attention due to their potential for higher energy efficiency and superior control performance compared to centralized configurations [5, 6]. A prominent solution in this category is the electro-hydrostatic actuator (EHA), which uses a variable-speed electric motor as the prime mover for each hydraulic actuator. Many studies have been conducted on that solution. Qu applied an electro-hydrostatic variable speed drive system in a skid steer loader, achieving a steady-state energy efficiency of up to 59.9% [7]. Ge proposed a EHA driving by an asymmetric pump and the energy consumption during the entire boom cylinder loading cycle can be reduced by 75.0 % [8]. Guo proposed a variable speed drive steering system for wheel loaders, which reduced energy consumption by 22.8% compared with centralized systems [9].

However, in most EHA implementations, the hydraulic pump displacement remains fixed. This limitation forces the electric motor's operating points to be dictated directly by the external load, leading to relatively low system efficiency—particularly under high-torque, low-speed conditions. To address this challenge, several cooperative control strategies for simultaneous speed and displacement adjustment have been proposed. Huang proposed an active load-sensitive EHA with a dual control variable system. The output flow of the pump is implemented by adjusting the motor speed and the pump displacement based on the load-sensitive principle. The system efficiency is optimized in real time and the system dynamic performance is improved [10, 11]. Lin developed a combined motor speed and hydraulic pump displacement control strategy, achieving hierarchical system pressure control, reducing energy consumption by up to 70% [12].

Nevertheless, existing methods predominantly rely on simplified rule-based approaches, which fail to achieve optimal system energy efficiency. Moreover, these strategies often neglect system dynamic characteristics, thereby limiting their practical effectiveness. The dynamic programming (DP) algorithm is a well-established method for solving global optimization problems in dynamic systems [13, 14]. However, its high computational burden renders it unsuitable for real-time implementation.

In this context, this paper proposes an energy-optimized control strategy for the work function of electric wheel loaders, based on cooperative variable speed and displacement control. The DP algorithm is first applied offline to derive efficiency-optimal operating parameters under typical working cycles. These results then guide the design of a real-time optimization strategy that incorporates system dynamics. The rest of the paper is organized as follows. Section II presents system mathematical modelling, section III shows DP algorithm and real-time optimization strategy, section IV presents simulation study and section V gives conclusions.

2. MATHEMATICAL MODELLING OF ELECTRO-HYDRAULIC ACTUATOR SYSTEM

2.1. System Overview

The schematic of EHA system with variable speed and pump displacement control for wheel loaders is shown in Figure 2.1. It uses an electric motor (EM) as a primary mover for each

hydraulic working function and is able to optimize the working points of both electric motor and hydraulic pump (HP). The working hydraulic system consists of lift and tilt functions. The hydraulic variable displacement pumps can work in four quadrants. Two 4/3 directional valves (DV) allow for load holding capability. An on-off valve works as a bypass valve (BPV) parallel to the tilt cylinder (TC). The accumulators (ACC) compensate for the differential flow of the cylinders during extension phase and intake excess flow during retraction phase. Two sets of pilot check valves (PCV) control the charging and discharging process of the accumulator.

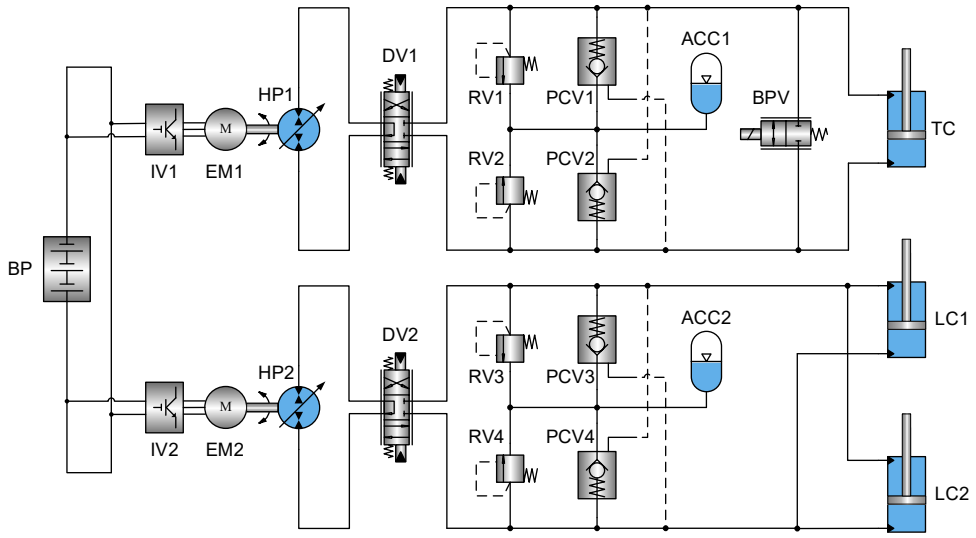

Figure 2.1. Schematic of electro-hydraulic actuator system with variable speed and pump displacement control

2.2. System Modelling

The physical-based mathematic models are established in this study for the following power optimization strategy design, including the models of battery pack, electric motors, hydraulic pumps, and so on. The SI unit is used in the mathematic models.

Battery Pack

A widely used equivalent circuit model composed of a voltage source, U_{oc}, and a resistance, R_b, is used for battery modelling [15,16]. The battery charge/discharge current, I_b, is given by:

$$I_b = \frac{U_{oc} - \sqrt{U_{oc}^2 - 4R_b P_{bout}}}{2R_b} \tag{2.1}$$

where P_{bout} is the output power (electric load power) of battery and can be expressed as:

$$P_{bout} = P_{iv1} + P_{iv2} \tag{2.2}$$

where P_{iv1}, and P_{iv2} are the input power of two inverters respectively.

Electric Motor

The electric motors in this study are permanent magnet synchronous motors (PMSM) that can work either as motors or as generators. A commonly used mathematical model of PMSM is to present electromagnetic vectors in an orthogonal d-q coordinate with d axis coinciding rotor flux linkage direction [17]. The winding stator voltage components in the d-q axis, u_d, u_q are:

$$\begin{cases} u_d = R_s i_d + \frac{d\psi_d}{dt} - \omega_{em}\psi_d \\ u_q = R_s i_q + \frac{d\psi_q}{dt} + \omega_{em}\psi_q \end{cases} \quad (2.3)$$

where R_s is stator winding's equivalent resistance, ω_{em} is the shaft speed of electric motor, i_d and i_q are equivalent currents in the d-q axis, ψ_d and ψ_q are d-q components flux linkage.

The electric motor output shaft torque T_{em} is:

$$T_{em} = \frac{3}{2} n_p i_q \left[\psi_f + (L_d - L_q) i_d\right] \quad (2.4)$$

where n_p is the number of pole pairs of motor stator.

The dynamics of electric motor shaft speed is:

$$(J_{em} + J_{hp})\dot{\omega}_{em} = T_{em} - T_{hp} - k_{vf}\omega_{em} \quad (2.5)$$

where J_{em} and J_{hp} are shaft inertia of electric motor and hydraulic pump, T_{hp} is hydraulic pump torque, k_{vf} is rotary friction coefficient.

Hydraulic Pump

The shaft torque of hydraulic pump, T_{hp}, is:

$$T_{hp} = \frac{D\Delta p}{\eta_{mech}{}^{\beta}} \quad (2.6)$$

where D is pump displacement, Δp is pressure difference between pump outlet and inlet pressure, η_{mech} is pump mechanical efficiency, β is mode factor ($\beta = 1$ in pumping mode and $\beta = -1$ in motoring mode).

The pump output flow rate, q_{hp} is:

$$q_{hp} = D\omega_{em}\eta_{vol}{}^{\beta} \quad (2.7)$$

where η_{vol} is pump volumetric efficiency.

3. DYNAMIC PROGRAMMING ALGORITHM AND REAL-TIME STRATEGY

3.1. Dynamic Programming Algorithm

The Dynamic Programming is a powerful algorithmic technique for solving complex optimization problems by breaking them down into simpler, overlapping subproblems. Its core principle is to solve each subproblem only once, store the solution, and reuse it when needed, thereby avoiding redundant calculations and improving efficiency, as shown in Figure 3.1. This "divide-and-conquer-with-memorization" approach is particularly effective for sequential decision-making processes. The method relies on Bellman's principle of

optimality, which states that an optimal policy consists of optimal sub-policies. By recursively defining the value of a state based on subsequent states, DP constructs an optimal solution from back to front, making it ideal for applications like pathfinding, resource allocation, and optimal control strategies.

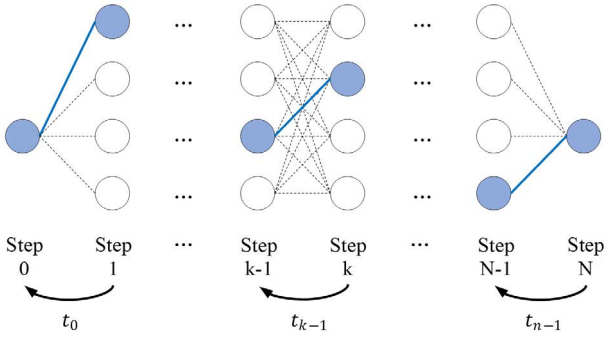

Figure 3.1. Schematic of dynamic programming algorithm

DP is adopted in this paper to obtain the efficiency-optimal operating parameters (rotary speed of electric motor and pump displacement) under typical working conditions of wheel loaders. Considering that the calculation complexity of DP algorithm increases exponentially with the dimensions of state variables and control variables, the pressure dynamics in the pipelines are neglected for simplicity and feasibility.

The flow chat of dynamic programming algorithm is shown in Figure 3.2. After getting the piston velocity and load force from loading cycle, the system operating mode is classified. The operating mode of wheel loaders normally includes two quadrants since the load force direction remains the same.

During extension mode ($v > 0$), the system power losses are given by:

$$P_{pvl} = \Delta p \omega_{em} D(1-\eta_{vol}) = \Delta p \frac{A_{head}}{\eta_{vol}}(1-\eta_{vol})v \quad (2.8)$$

$$P_{pml} = \Delta p \omega_{em} D \frac{1-\eta_{mech}}{\eta_{mech}} = \Delta p \frac{A_{head}}{\eta_{vol}} \frac{1-\eta_{mech}}{\eta_{mech}} v \quad (2.9)$$

$$P_{ml} = \omega_{em} T_{hp} \frac{1-\eta_{em}}{\eta_{em}} = \Delta p \frac{A_{head}}{\eta_{vol}\eta_{mech}} \frac{1-\eta_{em}}{\eta_{em}} v \quad (2.10)$$

$$P_{bl} = I_b^2 R_b \quad (2.11)$$

where P_{pvl} and P_{pml} are volumetric and mechanical power losses of hydraulic pump, P_{ml} is power loss of electric motor and inverter, P_{bl} is power loss of battery.

During retraction mode ($v < 0$), the system operations between lift and tilt functions are different. The lift function recoveries gravitational potential energy of loader working device and its hydraulic pump works in motoring mode. The system power losses are given by:

$$P_{pvl} = \Delta p A_{head}(1-\eta_{vol})v \quad (2.12)$$

$$P_{pml} = \Delta p A_{head}(1-\eta_{mech})\eta_{vol} v \quad (2.13)$$

$$P_{ml} = \Delta p A_{head}\eta_{vol}\eta_{mech}(1-\eta_{em})v \quad (2.14)$$

$$P_{bl} = I_b^2 R_b \tag{2.15}$$

For the tilt function, the bypass valve placed in parallel to the tilt cylinder is open during retraction mode to accelerate the motion process. Since the pressure difference between pump outlet and inlet pressure equals to zero, the system power losses during the bucket retracting are neglected.

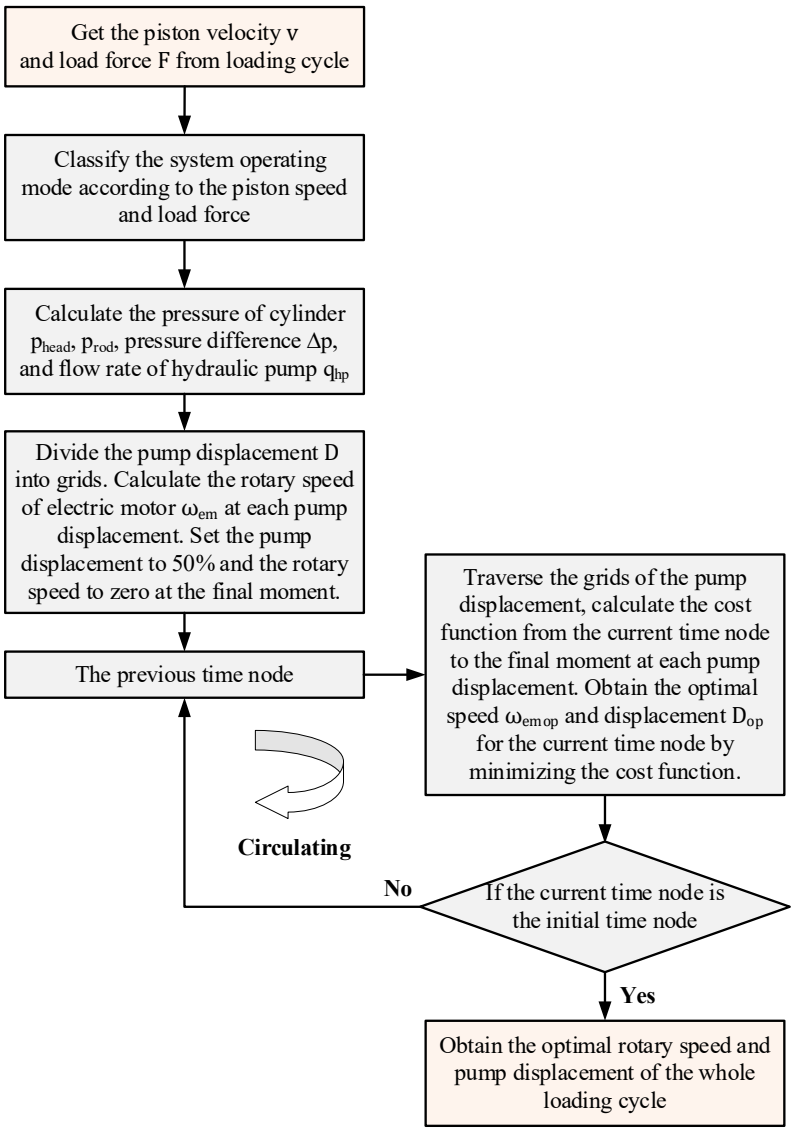

Figure 3.2. Flow chat of dynamic programming algorithm

After calculating the system states, a set of pump displacement is selected from 2.5 cc/rev to 250 cc/rev (100% maximum displacement) with an interval of 2.5 cc/rev. Then the rotary speed of electric motor at each pump displacement is calculated according to Eq. (2.7). To

facilitate the DP algorithm to find the optimal displacement more quickly, the pump displacement at the final moment is set to 50%. The rotary speed at the final moment is set to zero.

During the dynamic programming process, the rotary speed, acceleration of electric motor and the rate of change of the pump displacement should be restricted within proper range according to the real dynamics of electric motor and hydraulic pump. Therefore, a penalty function is added to the optimization problem to discard the state exceeding physical limitations in the optimization process, since a larger value from penalty function will be added besides cost function.

By setting the weight coefficient of all constraints. The expression of the penalty function is given by:

$$\begin{aligned} f_{pen} = k_{penalty}\big[&H(\omega_{em} - \omega_{emmax}) + H(\omega_{em} - \omega_{emmin}) + H(\dot{\omega}_{em} - \dot{\omega}_{emmax}) + \\ &H(\dot{\omega}_{em} - \dot{\omega}_{emmin}) + H\big(\dot{D} - \dot{D}_{max}\big) + H\big(\dot{D} - \dot{D}_{min}\big)\big] \end{aligned} \tag{2.16}$$

$$\dot{\omega}_{emmax} = \frac{T_{emmax}\text{-}T_{hp}\text{-}k_{vf}\omega_{em}}{J_{em}+J_{hp}} \tag{2.17}$$

$$\dot{\omega}_{emmin} = \frac{T_{emmin}\text{-}T_{hp}\text{-}k_{vf}\omega_{em}}{J_{em}+J_{hp}} \tag{2.18}$$

where $k_{penalty}$ is weight coefficient of penalty function, ω_{emmax} and ω_{emmin} are the maximum and minimum rotary speed of electric motor, $\dot{\omega}_{emmax}$ and $\dot{\omega}_{emmin}$ are the maximum and minimum rotary acceleration of electric motor, T_{emmax} and T_{emmin} (reverse) are the maximum and minimum output shaft torque of electric motor, $\dot{D}_{max}$ and $\dot{D}_{min}$ are the maximum and minimum rate of change of the pump displacement obtained from test results.

The cost function from the current time node to the final moment at each pump displacement is given by:

$$J_k = \int_{kT_s}^{(k+1)T_s} P_{pvl} + P_{pml} + P_{ml} + P_{bl}dt + f_{pen,k} + J_{k+1} \tag{2.19}$$

where J_k, J_{k+1} are cost functions of time nodes k and $k+1$, T_s is discrete-time timestep.

By traversing the grids of the pump displacement, the optimal pump displacement for the current time node is obtained by minimizing the cost function:

$$D_{op,k} = \underset{D \in \Omega}{\operatorname{argmin}}\, J_k \tag{2.20}$$

The nested loops are used that start at the end and the optimal pump displacement is computed for every node recursively.

3.2. Real-Time Rotary Speed and Pump Displacement Optimization Strategy

Although DP is an effective method to solve global optimization problems, its substantial computational demands make real-time optimization infeasible. Therefore, in this paper, a real-time rotary speed and pump displacement optimization strategy is designed based on the optimized results from dynamic programming algorithm.

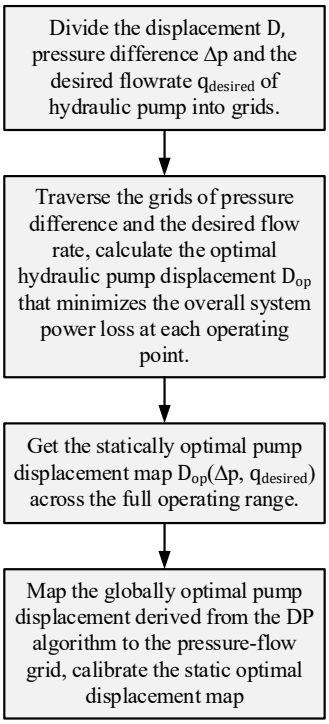

Figure 3.3. Flow chat of real-time optimization strategy

The flow chat of real-time optimization strategy is shown in Figure 3.3. The real-time optimization strategy is a two-stage methodology for determining the globally optimal displacement of a hydraulic pump. The first stage is to obtain the statically optimal pump displacement map $D_{op}(\Delta p, q_{desired})$ across the full operating range. Key operational parameters (displacement D, pressure difference Δp, and desired flow rate $q_{desired}$ of hydraulic pump) are discretized into grids in the beginning. For each discrete operating point within this grid, it calculates the specific pump displacement that minimizes the overall system power loss. This exhaustive search yields a preliminary, statically optimal displacement map, which defines the most efficient pump setting for any given pressure and flow requirement within the predefined operating range.

In the final and crucial step, the results from DP algorithm, which computes a sequence of optimal decisions over time, are mapped onto the same pressure-flow grid. This integration allows the static map to be calibrated and refined with the globally optimal trajectory from the DP solution, thereby enhancing its accuracy and ensuring system-wide optimality.

4. SIMULATION STUDY

4.1. Simulation Parameters

The dynamic simulation model of the proposed system is developed in Amesim. The simulation models target a 12 tons electric wheel loader. The major parameters are shown in Table 4.1. The nominal voltage of battery is 648 V. The accumulator volume is calculated to compensate for the differential volume of the cylinders during extension phase. The

displacement of the hydraulic pumps determines the shaft speed limits of electric motors. In the simulation, two 22 L accumulators are selected for the tilt and lift functions.

The efficiency map of electric motor is obtained from the experimental data as shown in Figure 4.1. The flowrate and shaft torque of hydraulic pump/motor is shown in Figure 4.2 and Figure 4.3. The first loading cycle used in this study is 60 s long and includes six phases: preparing, bucket filling, load holding, boom lifting, dumping and boom lowering.

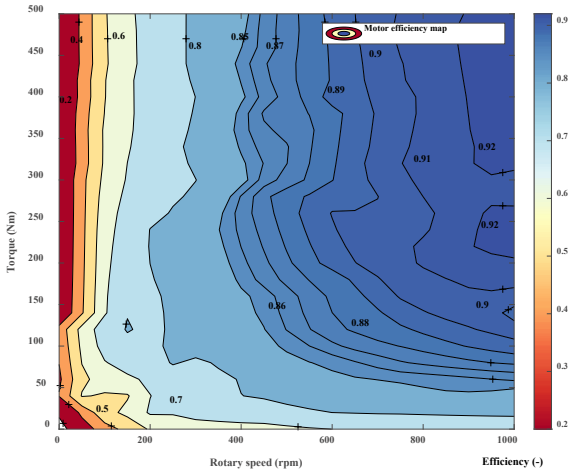

Figure 4.1. Efficiency map of the electric motor

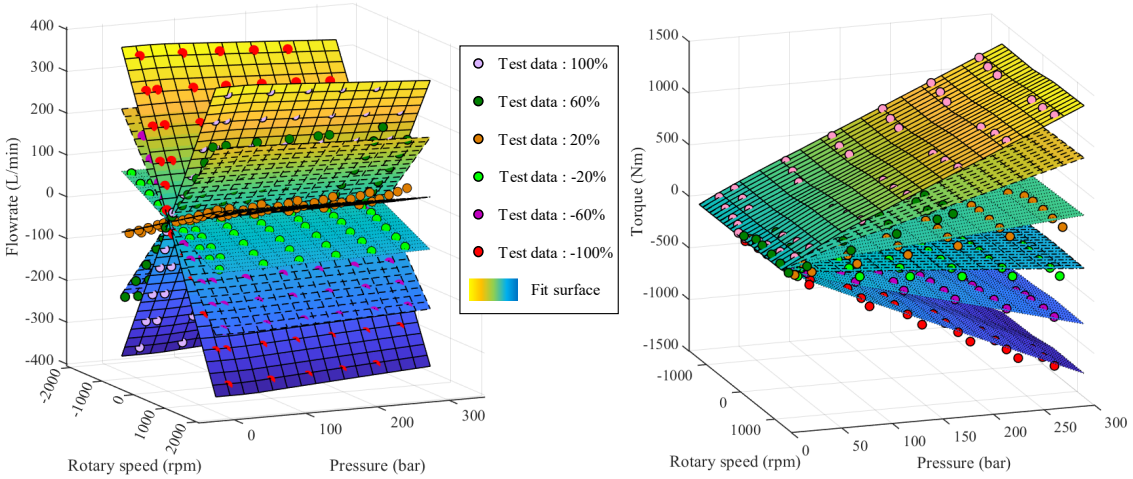

Figure 4.2. Flowrate and shaft torque of hydraulic pump/motor

Table 4.1. Main simulation parameters

Property		**Value**	**Unit**
Battery	Nominal voltage	648	V
Electric motor	Maximum rotary speed	2000	rpm
	Maximum torque	648	Nm
Hydraulic pump	Geometric displacement	250	cc/rev

Accumulator	Volume	22.0	L
	Precharge pressure	8	bar
Direction valve	Maximum throttling area	256.12	mm2
	Natural frequency	20.0	Hz
	Damping ratio	1.2	-
Tilt/Lift cylinder	Piston stroke	350.0/450.0	mm
	Piston diameter	180.0/150.0	mm
	Rod diameter	80.0/90.0	mm

4.2. Simulation Results

There are three hydraulic system configurations considered in the simulation study: normal EHA system, variable speed and pump displacement control system with DP algorithm (VSVD-DP), variable speed and pump displacement control system with real-time optimization strategy (VSVD-RT).

In the EHA system, each actuator is driven by a stand-alone electric motor with a fixed displacement hydraulic pump and the actuator speed is controlled through variable speed drive of electric motor. The 4/3 directional valve is fully open when the actuator moves and closes in standby mode. The comparison of piston displacement between three systems is shown in Figure 4.3. The piston displacements of the three systems are essentially consistent, except for the discrepancy during the bucket lowering phase. This is due to the drastic changes in piston velocity during the bucket lowering phase, which poses challenges to the control accuracy of variable speed and displacement system.

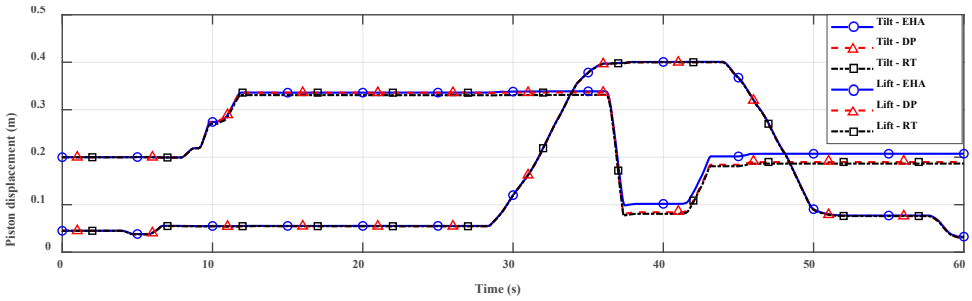

Figure 4.3. Comparison of piston displacement between three systems

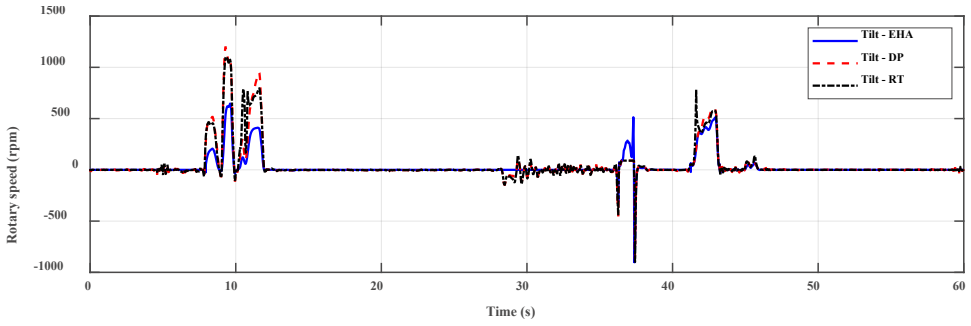

Figure 4.4. Comparison of tilt rotary speed between three systems

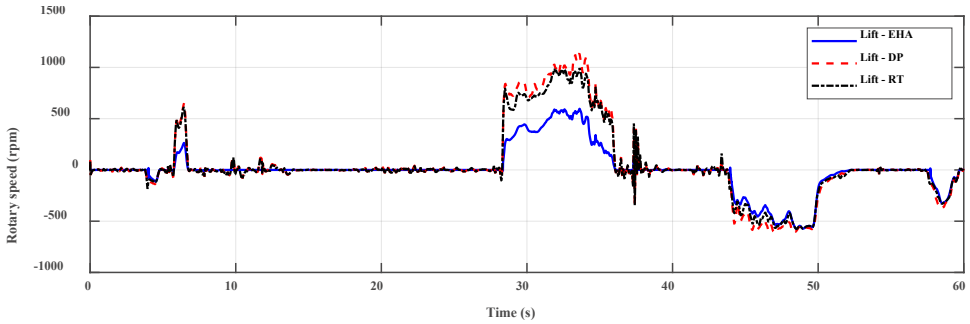

Figure 4.5. Comparison of lift rotary speed between three systems

The comparison of rotary speed between three systems is shown in Figure 4.4 and Figure 4.5. As the 4/3 directional valve opens and closes during system status switching process, there are some pressure shocks leading to the peak fluctuations of motor shaft torque in the EHA system. Compared with the EHA system, the shaft speeds of DP and RT systems are much higher during bucket filling and boom lifting phase.

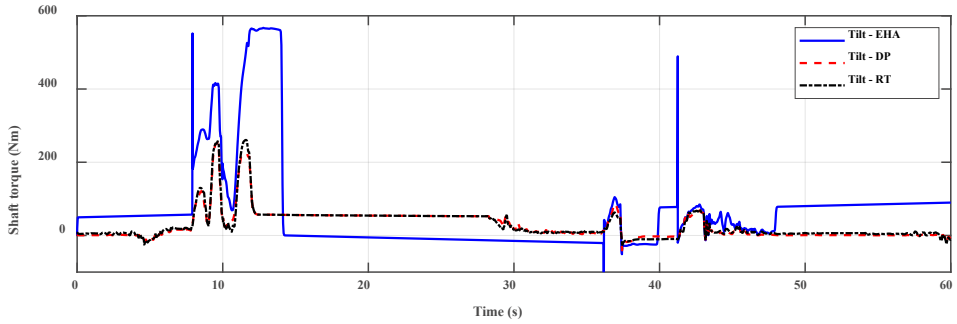

Figure 4.6. Comparison of tilt shaft torque between three systems

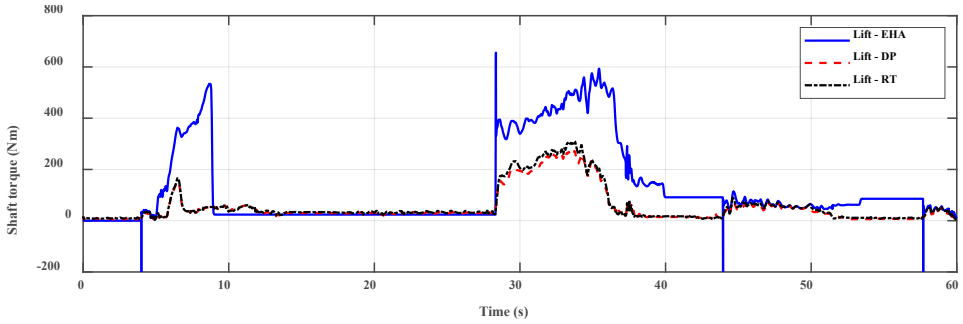

Figure 4.7. Comparison of lift shaft torque between three systems

The shaft torque results are shown in Figure 4.6 and Figure 4.7. Due to the reduction in hydraulic pump displacement, the motor output torque of the DP and RT systems in operating mode decreases significantly compared with EHA system. The pump displacement results between three systems are shown in Figure 4.8 and Figure 4.9. The pump displacement in the EHA system is always maintained at 100%, while the pump

displacement in the DP and RT systems is adjusted in real time according to operating conditions. By adjusting the pump displacement, the operating points of the motors in the DP and RT systems shift toward the high-efficiency region characterized by high speed and low torque. The 4/3 directional valves in the DP and RT systems are fully open from the beginning to the end. In the standby mode, both DP and real-time strategies keep the pump displacement close to zero to reduce the power loss of electric motor.

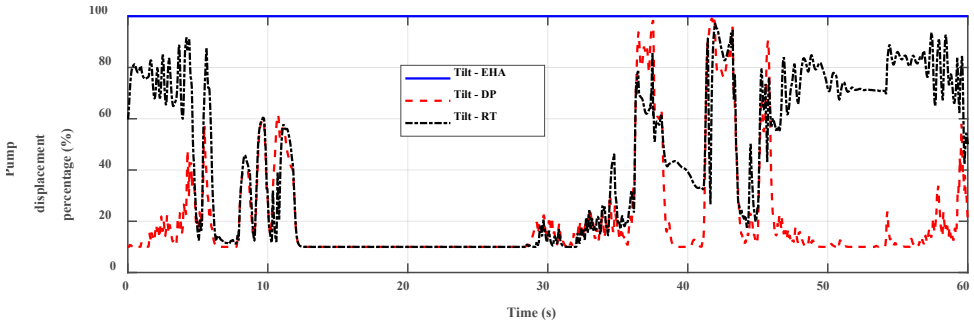

Figure 4.8. Comparison of tilt pump displacement between three systems

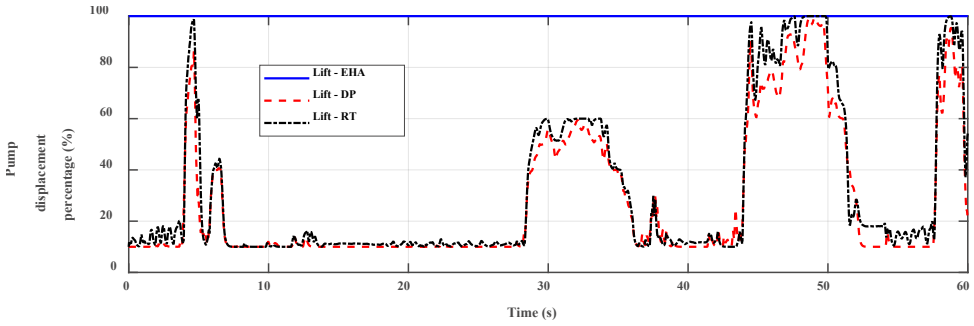

Figure 4.9. Comparison of lift pump displacement between three systems

The pump displacement percentage curves between DP and RT systems still have slight differences. Since the DP strategy accounts for dynamic constraints of the system, the obtained globally optimal displacement percentage exhibits smoother variations. In contrast, the real-time optimization strategy leads to more fluctuations. However, owing to the calibration of the real-time strategy based on DP results, the pump displacement from RT system is close to the results from DP with much smaller computational complexity.

The comparison of energy consumption between EHA, DP, optimized and non- optimized RT systems is shown in Figure 4.10. The total energy consumptions of these system are 218.3 kJ, 197.0 kJ, 198.4 and 202.9 kJ respectively. Compared with the EHA system, the energy consumptions of VSVD systems are reduced, primarily due to the decrease in electric motor energy loss. The DP system achieves the lowest energy consumption through offline global optimization. Compared to the EHA system, the non-optimized RT system saves 7.05% in energy consumption, while a 9.12% reduction is achieved in the optimized RT system, approaching the optimal result of the DP system.

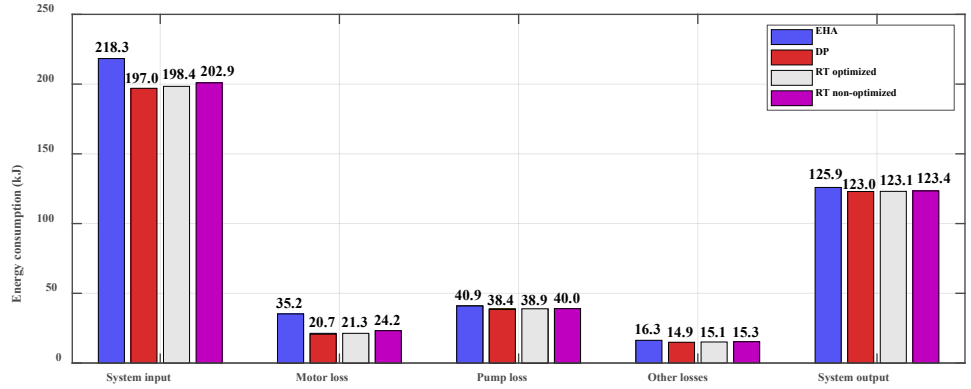

Figure 4.10. Comparison of energy consumption between systems

The aforementioned results verify the energy-saving effectiveness of the real-time optimization strategy under specific operating conditions. To investigate the influence of different operating conditions on the proposed method, an unfamiliar loading cycle lasting 32 s is selected as the system input. The hydraulic cylinder piston displacement curve under the new cycle is shown in Figure 4.11. Compared with the previous cycle, the piston displacement variation is greater, and the intervals between movements are shorter.

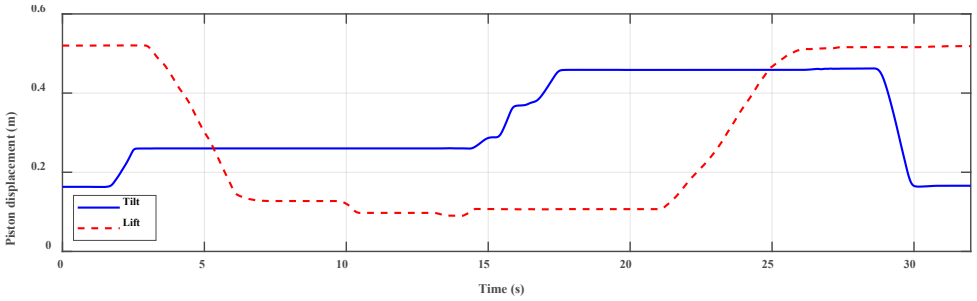

Figure 4.11. Piston displacement under 32 s long loading cycle

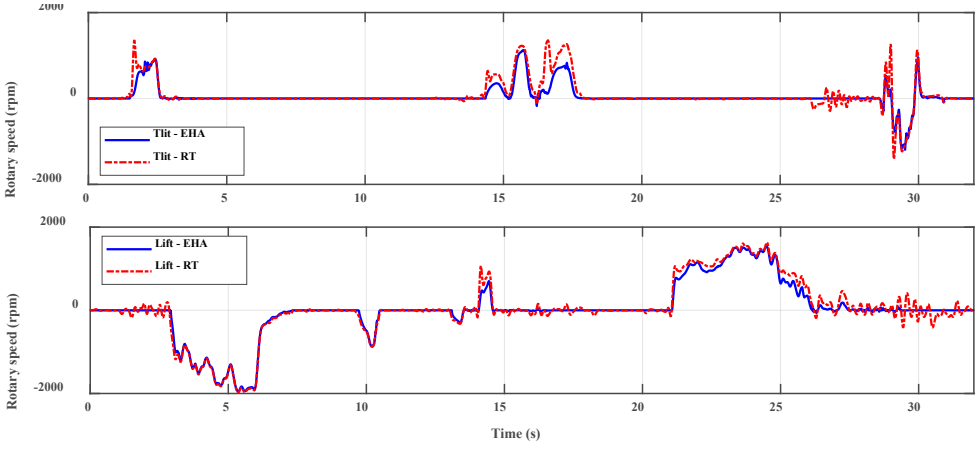

Figure 4.12. Comparison of rotary speed between EHA and RT systems

The comparison of rotary speed between EHA and RT systems is shown in Figure 4.12. The shaft speed of RT system is slightly higher than that of the EHA system. From the results of lift working function, it can be observed that when the cycle requires high flowrate, the motor rotary speeds of the EHA and RT systems are essentially the same, indicating that the hydraulic pump operates at full displacement under such conditions.

The comparison of shaft torque between EHA and RT systems is shown in Figure 4.13. The mean motor shaft torque of the RT system is significantly lower than that of the EHA system. The RT optimization strategy can rapidly reduce motor torque by adjusting the hydraulic pump displacement after the operation is completed, thereby minimizing motor energy loss.

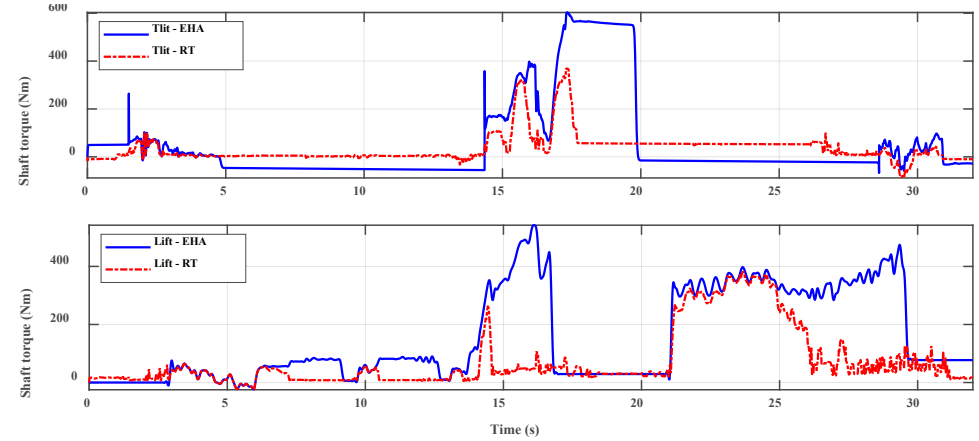

Figure 4.13. Comparison of shaft torque between EHA and RT systems

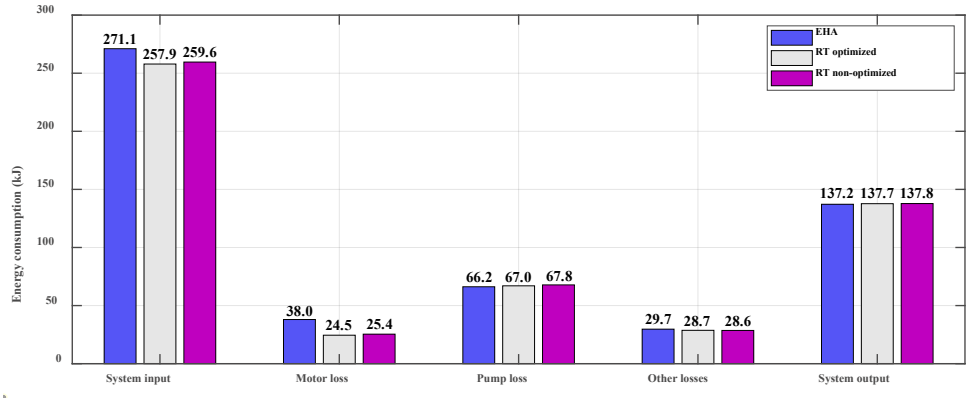

Figure 4.14. Comparison of energy consumption between EHA and RT systems

The comparison of energy consumption between EHA, optimized and non- optimized RT systems is shown in Figure 4.14. The total energy consumptions of these system are 271.1 kJ, 257.9 kJ and 259.6 kJ respectively. Both VSVD systems have smaller energy consumptions than that of the EHA system under an unfamiliar loading cycle. Due to the increased power output required for short loading cycle, the operating time under full hydraulic pump displacement is extended in the VSVD systems, resulting in a reduced margin of energy consumption reduction compared to the EHA system. Although the new

cycle shortens the overall time with an increased piston displacement change, the motion pattern of the working functions remains similar to that of the long cycle. Consequently, the optimized RT strategy achieves additional system energy savings compared to the non-optimized one.

5. CONCLUSIONS

In this paper, a power optimization strategy for electric wheel loader work function with variable speed and pump displacement cooperative control is proposed. The dynamic programming algorithm is applied offline to obtain the efficiency-optimal operating parameters under typical working conditions of wheel loaders. Based on the optimized results, a real-time rotary speed and pump displacement optimization strategy is designed.

The dynamic simulation models of three hydraulic systems (EHA, VSVD-DP, VSVD-RT) are developed in Amesim. Two loading cycles are used in this study. Under the familiar cycle, VSVD-RT system achieves a 9.12% reduction in total energy consumption compared with the EHA system (9.76% for DP system). Under another unfamiliar cycle, the proposed system still has a 4.9% energy consumption reduction. The results indicate that the real-time optimization strategy possesses energy-saving potential across various operating conditions. In practical applications, the real-time model can be calibrated using DP global optimal solutions derived from multiple frequently-used loading cycle, thereby enhancing its adaptability to different operating scenarios.

6. REFERENCES

[1] H. Assaf, S. Sarode, A. Vacca A, et al, 'Electric machine sizing consideration for ePumps in mobile hydraulics', Energy science & engineering, vol.12, no. 3, pp.793-809, 2024.

[2] Z. Quan, L. Ge, Z. Wei, et al, 'A Survey of Powertrain Technologies for Energy-Efficient Heavy-Duty Machinery', Proceedings of the IEEE, vol. 109, no. 3, pp. 279-308, 2021.

[3] B. Xu, M. Cheng, 'Motion control of multi-actuator hydraulic systems for mobile machineries: Recent advancements and future trends', Front Mech Eng, vol. 13, no. 2, pp. 151-166, 2018.

[4] D. B. Beck, D. E. Fischer, D. G. Kolks, et al, 'Novel system Architectures by individual drives', In: 10th Int Fluid Power Conf, pp. 29-62, 2016.

[5] J. Lodewyks, P. Zurbrügg, 'Decentralized energy-saving hydraulic concepts for mobile working machines', In: 10th Int Fluid Power Conf, pp. 79-90, 2016.

[6] X. He, H. Liu, S. He, et al, 'Research on the energy efficiency of energy regeneration systems for a battery-powered hydrostatic vehicle', Energy, vol. 178, pp. 400-418, 2019.

[7] S. Qu, D. Fassbender, A. Vacca, et al, 'A high-efficient solution for electro-hydraulic actuators with energy regeneration capability', Energy, vol. 216, pp. 119291, 2021.

[8] L. Ge, L. Quan, Y. Li, et al, 'A novel hydraulic excavator boom driving system with high efficiency and potential energy regeneration capability', Energy Convers Manag, vol. 166, pp. 308–17, 2018.

[9] T. Guo, B. Wu, T. Lin, et al, 'Closed-Circuit Pump-Controlled Electro-Hydraulic Steering System for Pure Electric Wheel Loader', Applied Sciences-Basel, vol. 12, no. 11, pp. 5740, 2022.

[10] L. Huang, T. Yu, Z. Jiao, et al, 'Research on Power Matching and Energy Optimal Control of Active Load-Sensitive Electro-Hydrostatic Actuator', IEEE Access, vol. 9, pp. 51121-51133, 2021.

[11] L. Huang, T. Yu, Z. Jiao, et al, 'Active Load-Sensitive Electro-Hydrostatic Actuator for More Electric Aircraft', Applied Sciences, vol. 10, no. 19, pp. 6978-21, 2020.

[12] T. Lin, Y. Lin, H. Ren, et al, 'A double variable control load sensing system for electric hydraulic excavator', Energy (Oxford), vol. 223, pp. 119999, 2021.

[13] J. Nurmi, J. Mattila, 'Global energy-optimised redundancy resolution in hydraulic manipulators using dynamic programming', Automation in Construction, vol. 73, pp. 120-134, 2017.

[14] O. Sundstrom, D. Ambiihl, L. Guzzella, 'On implementation of dynamic programming for optimal control problems with final state constraints', Oil & Gas Science and Technology, vol. 65, no. 1, pp. 91-102, 2010.

[15] H. Zhang, F. Wang, B. Xu, et al, 'Extending battery lifetime for electric wheel loaders with electric-hydraulic hybrid powertrain', Energy, vol. 261, pp. 125190, 2022.

[16] F. Wang, Z. Wu, B. Xu, et al, 'A Mode-driven Control Strategy to Reduce Electric Drive Peak Power of Hybrid Wheel Loader Propulsion System', IEEE Transactions on Vehicular Technology, vol. 72, no. 5, pp. 5948-5961, 2023.

[17] S. H. Kim, 'Electric Motor Control: DC, AC, and BLDC Motors', 2017.

Biographies

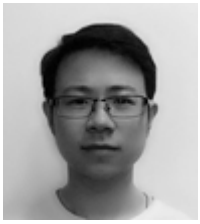

Jiaming Wu received B.S. degree in mechanical engineering from Zhejiang University, Hangzhou, China, in 2019. He is currently pursuing his Ph.D. degree in mechanical engineering at Zhejiang University, Hangzhou, China. His main research focuses on modeling and control of electro-hydrostatic actuator system for off-road vehicles.

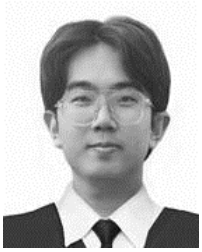

Yihan Qiao received B.S. degree in mechanical engineering from Zhejiang University, Hangzhou, China, in 2022. He is currently pursuing his Ph.D. degree in mechanical engineering at Zhejiang University, Hangzhou, China. His main research focuses on electro-hydraulic hybrid variable speed drive system for wheel loader.

Feng Wang received B.S., M.S., and Ph.D. degrees in mechanical engineering from Zhejiang University, Hangzhou, China, in 2003, 2005, and 2009.

In 2009 he became a Postdoctoral Associate in the Department of Mechanical Engineering at University of Minnesota, Minneapolis, MN, USA, where he joined the NSF Engineering Research Center for Compact and Efficient Fluid Power (CCEFP). In 2016 he became an Assistant Professor in the School of Mechanical Engineering at Zhejiang University, Hangzhou, China, where he joined the State Key Laboratory of Fluid Power and Mechatronics Systems. His research interests include modeling and control of intelligent hydraulic powertrains for heavy-duty vehicles and large utility wind turbines.

Bing Xu received Ph.D. degree in mechanical engineering from Zhejiang University, Hangzhou, China, in 2001. He is currently a Professor in the school of mechanical engineering and also the Director of the State Key Laboratory of Fluid Power Transmission and Control at Zhejiang University.

He has authored or co-authored more than 200 journal and conference papers, and authorized 49 patents. His research interests include fluid power components and systems, mechatronic systems design and motion control for mobile machinery. Prof. Xu is a Chair Professor of the Yangtze River Scholars Program and a science and technology innovation leader of the Ten Thousand Talent Program.